ELSEVIER

NeuroImage

www.elsevier.com/locate/ynimg
NeuroImage 25 (2005) 462–470

Connectivity exploration with structural equation modeling: an fMRI study of bimanual motor coordination

Jiancheng Zhuang,[a,b] Stephen LaConte,[a] Scott Peltier,[a] Kan Zhang,[c] and Xiaoping Hu[a,*]

[a]*Biomedical Imaging Technology Center, Department of Biomedical Engineering, Emory University/Georgia Institute of Technology, 1639 Pierce Drive, Suite 2001, Atlanta, GA 30322, USA*
[b]*Magnetic Resonance Imaging Unit, Department of Psychiatry, Columbia University, New York, NY 10027, USA*
[c]*Institute of Psychology, Chinese Academy of Sciences, Beijing, China*

Received 6 May 2004; revised 8 September 2004; accepted 3 November 2004
Available online 25 January 2005

The present fMRI study explores the connectivity among motor areas in a bimanual coordination task using the analysis framework of structural equation modeling (SEM). During bimanual finger tapping at different frequency ratios, temporal correlations of activations between left/right primary motor cortices (MI), left/right PMdc (caudal dorsal premotor area) and supplementary motor cortex (SMA) were detected and used as inputs to the SEM analysis. SEM was extended from its traditional role as a confirmatory analysis to be used as an exploratory technique to determine the most statistically significant connectivity model given a set of cortical areas based on anatomic constraints. The resultant network exhibits coupling from left MI to right MI, links from both PMs to the two MIs, a negative interaction from left PM to right PM, and functional influence from SMA to right MI and right PM, revealing contributions of these areas to bimanual coordination.

Keywords: Functional magnetic resonance imaging; Bimanual motor coordination; Structural equation modeling; Effective connectivity

Introduction

The coupling or interference between dual motor tasks by two hands is familiar in our daily experience and has been investigated in many psychophysical and MEG experiments (Chan and Chan, 1995; Franz et al., 1991; Jirsa et al., 1998; Mayville et al., 2001; Tuller and Kelso, 1989; Yamanishi et al., 1980). For example, in an experimental study on spatial coupling of dual motor tasks (Chan and Chan, 1995), participants were asked to perform continuous simultaneous drawing of circles and straight lines using both hands simultaneously. There was a strong tendency for the line to become more circle-like and the circle to become more line-like, as measured by orientation ratio (i.e., height/width) of the circle or line. Such phenomena were termed a spatial magnet effect, and such interference was referred to as "coupling" between the left and right motor systems (Franz et al., 1991; Kelso et al., 1988).

In addition to the interaction described above, the frequency ratios (between two hands) for which polyrhythmic bimanual movement is stable were found to follow a Farey series. Specifically, with a/b and c/d as two base levels of stable frequency ratios, the ratio $(a + b) / (c + d)$ produces the frequency ratio for the next level of (decreased) stability (Treffer and Turvey, 1993). In the experiments of bimanual circle/line drawing task described above, it was shown that the spatial coupling (or interference, i.e., the deviation of orientation ratio of the drawn circles from that of the perfect circle) was the strongest at the ratio of 1/1 (Level 0), the second strongest at 1/2 (Level 1), and the third strongest at 2/3 (Level 2) (Chan and Chan, 1995).

In the context of similar bimanual coordination tasks, such as anti-phase vs. in-phase hand movement or poly-rhythmic finger tapping, recent functional imaging studies (Debaere et al., 2003, 2004; De Weerd et al., 2003; Immisch et al., 2001; Jancke et al., 2000; Koeneke et al., 2004; Sadato et al., 1997; Toyokura et al., 1999) indicated strong involvement of SMA in motor coordination between two hands. The role of premotor area in the bimanual motor coordination was also studied in depth by fMRI (Debaere et al., 2003, 2004; De Weerd et al., 2003; Immisch et al., 2001; Koeneke et al., 2004; Sadato et al., 1997). In recent fMRI and electrophysiological studies (Debaere et al., 2003, 2004; De Weerd et al., 2003; Donchin et al., 1998; Koeneke et al., 2004; Toyokura et al., 1999), an interaction between contralateral primary motor cortices was found during bimanual coordination tasks. Subcortical structures such as basal ganglia and cerebellum were also found activated during bimanual tasks (Tracy et al., 2001; Debaere et al., 2003, 2004).

Two biological models of motor coordination attempted to explain these coupling phenomena (Cardoso de Oliveira, 2002; Debaere et al., 2003, 2004): generalized motor programs (GMP)

* Corresponding author. Fax: +1 404 712 2707.
E-mail address: xhu@bme.emory.edu (X. Hu).
Available online on ScienceDirect (www.sciencedirect.com).

1053-8119/$ - see front matter © 2004 Elsevier Inc. All rights reserved.
doi:10.1016/j.neuroimage.2004.11.007

and intermanual crosstalk model. The GMP was inspired by the strong tendency for spatiotemporal similarity of bimanual movements and proposed that there could be a common motor plan for both hands (Schmidt, 1975). In contrast to GMP, the theory of intermanual crosstalk generally suggested that the interactions between the movements of the two arms resulted from partial intermingling (crosstalk) between two independent manual motor plans (Marteniuk and MacKenzie, 1980). Alternatively, GMP could be applied in a hand-specific manner in which the two independent motor plans of the crosstalk model can be viewed as the lowest level of the GMP.

Despite this great body of work, the underlying neural network responsible for bimanual coordination is far from well understood; questions remaining to be answered include where the GMP is generated and whether there exists crosstalk between bilateral primary motor cortices, premotor areas and SMA (Cardoso de Oliveira, 2002; Kelso et al., 1988). Neural interactions, or interchanges of neuronal (electrical or chemical) signals between different brain sites, may be one of the keys to understanding these motor coordination phenomena (Sadato et al., 1997), given that most existing literature (De Weerd et al., 2003; Immisch et al., 2001; Jancke et al., 2000; Koeneke et al., 2004; Toyokura et al., 1999) indicates that bimanual motor coordination requires a group of cortical regions but does not provide detailed information on interactions and couplings between these regions.

Many challenges exist in the analysis of fMRI data to ascertain connectivity relationships across motor cortices during bimanual coordination tasks. First, the widely used correlation analysis across multiple spatial regions cannot reveal causal directions. This is because a correlation coefficient only indicates the degree with which two time courses co-vary with each other, but is not able to provide directional information on the interaction between these two regions. A second challenge is that the observed temporal latency of the BOLD response between different brain areas cannot be used to ascertain the temporal order of neural activities. This occurs because the local hemodynamic response, which depends on the local physiology, could be region specific, blur or delay the temporal evolution of BOLD signals, and make it unable to reflect the timing of neuronal events at different brain sites. Consequently, observed temporal differences in event-related paradigms are not reliable for retrieving information about the direction of the interaction. The third challenge is that many traditional analysis methods fail to provide a complete account of interactions if more than two brain regions are involved. When studying more than two regions, each one can interact with several other regions. One region can affect another directly or indirectly, i.e., passing through a third party in the model, and can be affected by several regions. As a result, correlation of two areas could include both direct and indirect effects, and a correlation analysis cannot tease these apart. For this kind of "many-body problem" in neural interactions, structural equation modeling provides a unique analysis framework.

Structural equation modeling (SEM) is a statistical technique that is able to examine causal relationships between multiple variables. SEM approaches the data differently from the usual statistical methods such as multiple regression or ANOVA. The parameters in the SEM model are connection strengths or path coefficients between different variables, which reflect the effective connectivity in our neural network model. Parameters are estimated by minimizing the difference between the observed covariances and those implied by a structural or path model. SEM was initially developed and applied in biology, psychology, economics, and other social sciences (Wright, 1920). In 1994, hypothesizing a connectivity model based on prior knowledge of anatomy and connectivity, McIntosh and Gonzalez-Lima (1994) applied SEM to PET data, demonstrating the dissociation between ventral and dorsal visual pathways in object and spatial vision. SEM was also used to characterize connectivity changes within the motor system of Parkinsonian patients (Grafton et al., 1994). Büchel and Friston (1997) used SEM analysis in an fMRI study to investigate the nonlinear interactions among V1, V5, posterior parietal cortex, and prefrontal cortex. More recently, Maguire et al. (2001) compared the structural equation models between human brains with and without bilateral hippocampal damages during a memory retrieval task.

To date, SEM has been used as a confirmatory analysis technique. Most existing studies only compare a couple of possible connectivity models derived from prior knowledge. But in the case when most connections are not known or the complexity of the anatomic network leads to a large number of possibilities, the traditional network analysis method cannot be applied. In this paper, we adapt SEM for exploratory analysis of fMRI data and demonstrate that such an analysis is capable of identifying the best model from an ensemble of all possible models using comprehensive sorting of multiple fit indices. This is demonstrated in the functional neural network for bimanual motor coordination, using a finger-tapping task involving two hands at two frequency ratios.

Materials and methods

fMRI experiment

Seven right-handed subjects participated in this study according to the guidelines set forth by the institutional review board at Emory University. Informed consent was obtained from all subjects. Of these, five were male and two were female with age range from 18 to 31 years, and subjects with life backgrounds that would lead to special motor skills, e.g., extensive training in piano, were excluded. Anatomical scans were acquired using a T1-weighted MPRAGE sequence (TI/TR/TE/Flip angle: 800 ms/25 ms/6 ms/15°; matrix: 256 × 256 × 140; FOV: 256 × 256 × 140 mm^3). Two oblique axial slices were acquired to cover the motor regions of interest. Data were acquired on a 3-T Siemens Trio whole body scanner using a gradient echo EPI sequence (TR/TE/Flip angle: 1 s/32 ms/90°; slice: 5.5 mm; matrix: 64 × 64; FOV: 20 × 20 cm^2). Subjects were visually cued to perform bimanual finger tapping at 1/1 (left and right index fingers at 2 Hz) or at 1/2 (left finger at 2 Hz and right finger at 4 Hz) ratios or unimanual tapping (2 Hz tapping either left only or right only). The slice prescriptions along with the sequence parameters were experimentally designed for anatomical coverage and to provide the additional benefit of a 2 Hz auditory pace arising from the imaging gradients. Subjects were allowed to practice the bimanual task prior to scanning and rested in a supine position inside the MR scanner during the imaging study, with their arms extended parallel to the trunk so that they could comfortably tap with the index fingers.

The bimanual tasks occurred in 40-s blocks of finger tapping alternated with 20-s intervals rest periods (without tapping), lasting for a total of 8 min (Fig. 1): Left(2/0)–Right(0/2)–

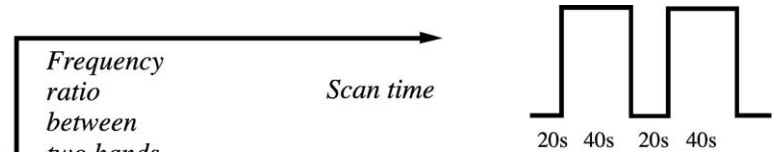

Bimanual Task

L	1	0	1	1	1	1	1	1
R	0	1	1	2	1	2	1	2

Unimanual Task

L	0	1	0	1	0	1	0	2
R	1	0	1	0	1	0	2	0

Fig. 1. Paradigm design. The columns represent the frequency ratio of tapping between left and right hands. The rows represent the temporal axis of experimental paradigm, and the boxcar shapes on the upper right show two basic blocks in the fMRI design.

L/R(1/1)–L/R(1/2)–L/R(1/1)–L/R(1/2)–L/R(1/1)–L/R(1/2). A second run was acquired with reversed temporal ordering [L/R(1/2)–L/R(1/1)–L/R(1/2)–L/R(1/1)–L/R(1/2)–L/R(1/1)–Right(0/2)–Left(2/0)]. In a third run, unimanual tapping was performed for the purpose of verification of bimanual behavioral performance and major functional motor areas, again with 40-s tapping and 20-s rest periods: Right (0/1)–Left(1/0)–Right(0/1)–Left(1/0)–Right(0/1)–Left(1/0)–Right(0/2)–Left(2/0).

Head motion was corrected and activated areas were detected using BrainVoyager (Maastricht, Netherlands). For each subject's bimanual data, activation maps were obtained using a *t*-test between all bimanual motor conditions [including L/R(1/1) and L/R(1/2)] and rest baselines, with statistical significance $P < 0.001$ and cluster size above 5 pixels.

Anatomical model

For SEM analysis, our regions of interests (ROIs) were chosen based on functional activation maps detected in the bimanual tasks (Fig. 2) and anatomical criteria outlined by neurological data in the literature (Baker et al., 1999; Roland and Zilles, 1996) as follows. ROIs were restricted to five major cortical motor areas: left/right MI, left/right dorsal premotor area and supplementary motor area (SMA). MI (Brodmann's area 4), i.e., primary motor cortex, was defined as the area anterior to the wall of the central sulcus and posterior to the midline of the precentral gyrus. The caudal dorsal premotor cortex (PMdc, Brodmann's area 6), often simply referred to as premotor cortex (PM), was defined as the area located caudally to the superior precentral sulcus, rostrally to the anterior wall of the precentral sulcus, and medially to the lateral part of the superior frontal gyrus (Dum and Strick, 1991; Roland and Zilles, 1996). The SMA was defined as the area caudally adjacent to the anterior lip of the precentral gyrus and laterally bordered by the medial part of the superior frontal gyrus.

With the above ROIs, all possible two-way interactions are considered in our exploratory analysis, except the paths starting from MIs because the primary motor cortices are assumed to be the end point of this network for the motor tasks used. Consequently, there are 14 anatomically available links (see Fig. 3). Any candidate model for effective connectivity for our task should be

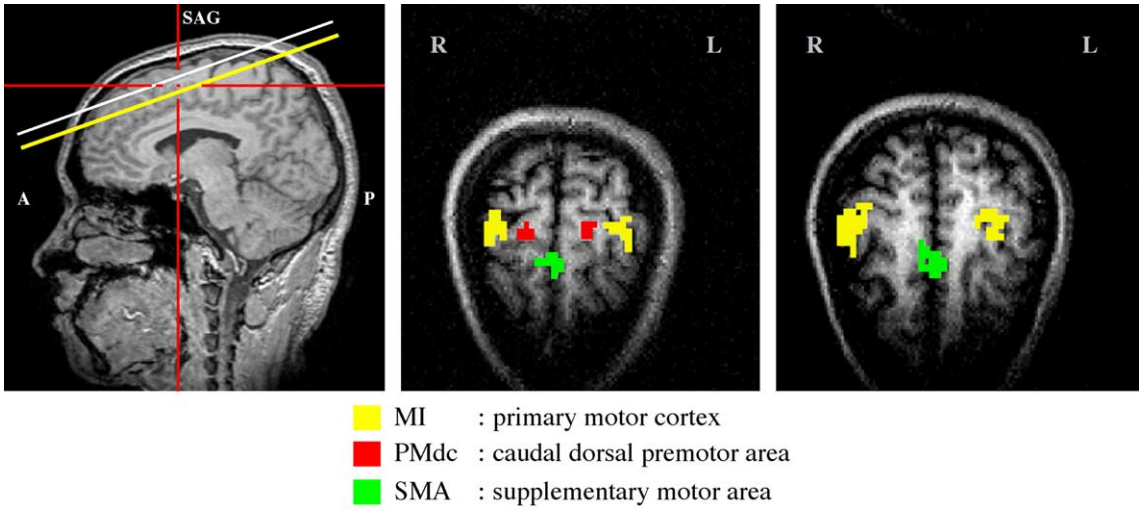

Fig. 2. The regions of interest (ROIs). Left: the slice position of functional MR images on a sagittal anatomical image. Right two: the selected ROIs based on typical activated areas detected in the bimanual coordination task, with different colors representing different motor cortices. The activation map was obtained using a *t*-test between all bimanual motor conditions and rest baselines with statistical significance $P < 0.001$.

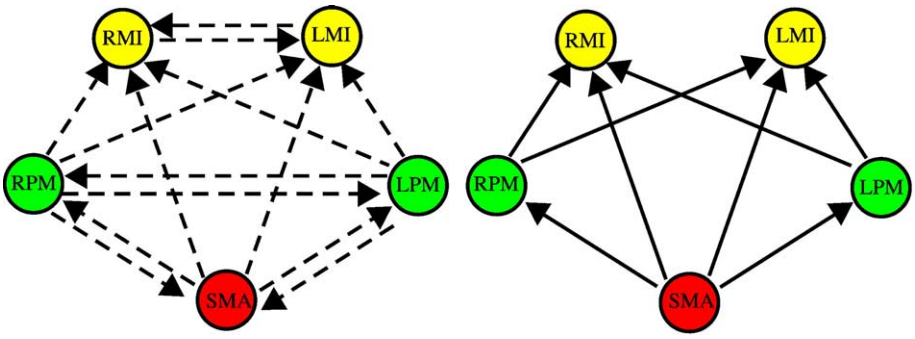

Fig. 3. All "probable" anatomic links (left) and a candidate model for SEM based on a combination of these links (right).

based on some combination of these anatomic connections. This leads to 2^{14} = 16,384 possible models.

Statistical methods

The average time courses from each spatial region were averaged within each temporal block (or experimental condition) to avoid the transient hemodynamic effect (Fig. 4), normalized into percentage scale by subtracting and then dividing by the mean, and finally concatenating both bimanual runs of every subject to create an intersubject time series for every ROI. The covariance matrix was calculated for the five observed variables (normalized, concatenated, ROI time series).

The 16,384 possible candidate models were automatically generated using custom software developed in Matlab (MathWorks, Natick, MA). One of these models is illustrated in Fig. 3. The SEM software Lisrel 8 (Jöreskog and Sorbom, Scientific Software International Inc., Chicago, IL) was used to estimate the statistical significance of each model fitting with the experimental data. The models were sorted by their performance indices as described below.

For the assessment of the overall model fit, goodness of fit index (GFI) and the adjusted goodness of fit index (AGFI) are most commonly used. AGFI is a more appropriate index of fit than GFI, in that AGFI accounts for the number of degrees of freedom in the model [see Eqs. (1) and (2); Byrne, 1994; Gerbing and Anderson, 1993; Hu and Bentler, 1999]. AGFI, however, does not adequately account for model complexity. We thus also used the parsimony goodness-of-fit index (PGFI), which is designed to measure the effects of the model complexity on fitting results [see Eq. (3)]. In our study, a lower PGFI threshold of 0.1 was used for the selection of fitted models. These indices are derived by

$$GFI = 1 - tr\left[\left(\sum{}^{-1} S - I\right)^2\right] \Big/ tr\left[\left(\sum{}^{-1} S\right)^2\right] \quad (1)$$

where tr indicates the trace operation, S is the covariance matrix, and Σ is the estimated S;

$$AGFI = 1 - [\,p(p+1)/2df](1 - GFI) \quad (2)$$

where p is the number of observations, and df is the degree of freedom in the model;

$$PGFI = (df/dfn)GFI \quad (3)$$

where dfn is the degree of freedom in the null model.

Another index for assessing overall model fit is the standardized residuals. The standardized residuals associated with a hypothesized model are also informal indices of fit (Byrne, 1994; Gerbing and Anderson, 1993). The largest residual indicates the overall degree of discrepancy in fitting the hypothesized and observed covariance matrices with larger values indicating greater discrepancy, and values approaching zero are desired.

Besides the overall fit indices, the reported t value of each path coefficient in the model should be greater than a certain critical value to reject the null hypothesis that the coefficient is 0. We used a path coefficient threshold of 0.10 ($t > 1.296$ and $P < 0.10$ with a degree of freedom above 60). Our nominal degrees of freedom are 7 subjects × 16 blocks × 2 runs = 224.

Based on these indices, our ranking method was summarized as follows. Models were eliminated from evaluation based on two statistical fit indices (evaluated with complexity index PGFI above 0.1 and t-test all paths significant below 90% confidence). Surviving models were first sorted based on AGFI and subsequently with the standardized residual.

Verification with improbable models

In addition to the candidate bimanual models, we demonstrate a verification of SEM by comparing with neurologically impossible or less probable models. Between each of these five nodes (ROIs), there should exist 5 × 4 = 20 directional links. Getting rid of 14 anatomically available paths, we are left with 20–12 = 6 "improbable" paths, as illustrated in Fig. 5, left. The number of models with these six paths is 2^6 = 64. The same SEM procedure used for "probable" models was applied to these "improper" models.

Reliability analysis via resampling

To assess the dependence of our results on the number of subjects, we performed an exhaustive resampling test. Specifically, subsets of data corresponding to one to six subjects were chosen from the original data set, using every possible combination of subjects. For example, there are seven possible combinations of six-subject data sets. Similarly, five-subject data sets have 21, etc. A confirmatory SEM was applied to each subset of data, using the top 5 models identified from our exploratory analysis of the seven-subject data set.

For each data subset, the five models were ranked using the procedure described above and scored with the Borda count method (Dym et al., 2002; Zwicker, 1991), e.g., the best model was given a score of 5, the second model a 4, etc. These scores were averaged for all combinations of a given subject number.

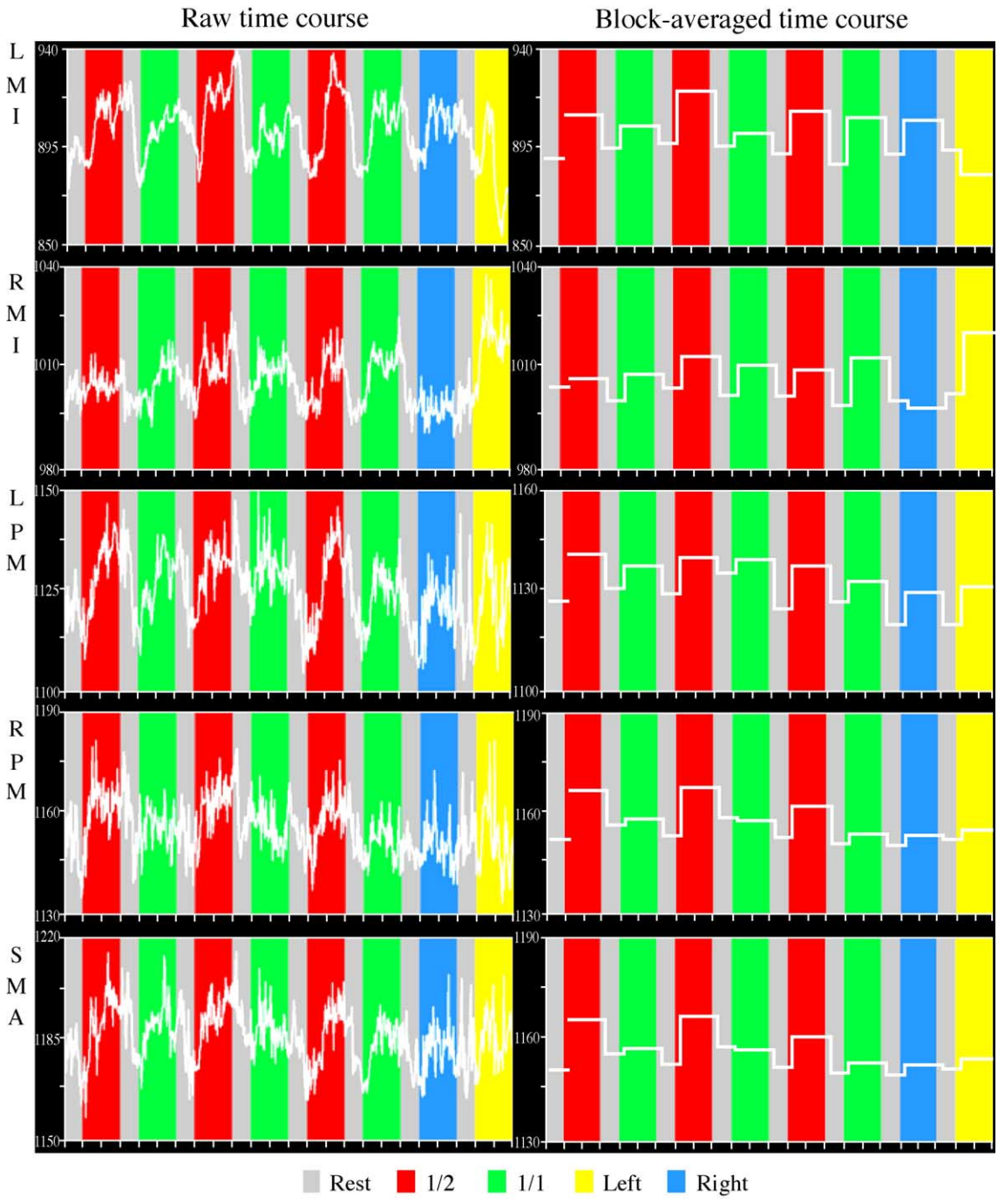

Fig. 4. Typical time courses (left) from five ROIs and their averages (right) for each task block.

For example, the Borda count numbers of six subjects were averaged among all seven combinations.

Results

In the bimanual task, the left and right primary motor cortices (MI areas) were robustly activated. The BOLD response in the left MI, corresponding to the movement of the right hand that interchanged between the 1/2 frequency ratio condition and 1/1 condition, was stronger at the 4 Hz rate than at the 2 Hz rate, as illustrated in Fig. 6. The BOLD signal in the left MI (LMI) averaged across all subjects in the bimanual tasks is approximately linear with the tapping frequency (green line in Fig. 6, $\text{Slope}_{\text{LMI, Bima}} = 0.73$) as that in the unimanual tasks (blue line, $\text{Slope}_{\text{LMI, Unima}} = 0.88$), consistent with previously published reports about the relationships between finger movement rate and fMRI signal changes (Rao et al., 1996: $\text{Slope}_{\text{LMI, Rao}} = 0.76$). Furthermore, the signal from the right MI (RMI) remains almost constant (Fig. 6, red line, $\text{Slope}_{\text{RMI, Bima}} = 0.12$) because the left hand was supposed to stay at 2 Hz tapping. Overall, Fig. 6 indicates that the subjects were following the instructions and accomplished the bimanual tapping at the desired

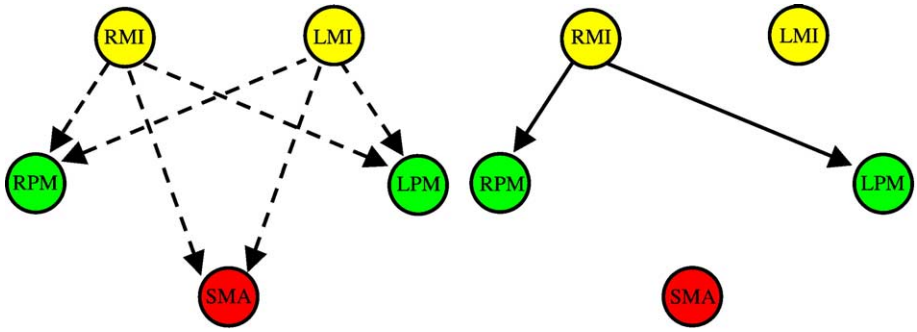

Fig. 5. Left: "Improbable" anatomic links, after omitting "probable" links in Fig. 3. Right: The "best" model in SEM based on a combination of these "improbable" links, which has the most significant fitting results.

frequency ratios with acceptable accuracy. As illustrated in the time courses in Fig. 4, different frequency ratios also elicited differential responses from the left and right PM areas, and the activation of SMA was highly correlated with both hands' movement and modulated by the task complexity.

With SEM calculations, the best-fitted structural equation model identified in bimanual task is shown in Fig. 7 (the path map) and Table 1 (the fitting results). The resultant model exhibits connections pointing to RMI directly from all other motor regions: LMI, L/R PM, and SMA. LMI received connection from right/left premotor cortices. The right premotor area has a supportive link from SMA and an inhibitive link from LPM.

For the best model, the GFI is almost 1.0, and the major sorting index AGFI is as high as 0.9995. The PGFI of this model has a very low value of 0.0667. The largest standardized residual, another sorting index, is 0.0257. The ratio of χ^2 and degree of freedom in the model is 0.0088, and the P value of χ^2 reaches the 0.925 level. The RMSEA value is close to 0, corresponding to a P value of 0.935. The t values of all path coefficients are above the threshold level of 1.296 associated with $P = 0.90$ significance, with most of them (6 of 8) reaching a statistical significance level of $P =$ 0.95. Other indices given by SEM also indicate an excellent fit (as seen in the fitting results Table 2). For example, the normed fit index (NFI) and the comparative Fit Index (CFI) of this model reached the maximum value of 1.00. All these provide strong evidence that the model fits the data well.

The resampling shows that the best-fit model from the seven-subject data is also consistently the highest-ranking model for data subsets consisting of four or more subjects (Table 3). In addition, the ranking for the six-subject data is the same as that of the seven-subject data, suggesting that the exploratory SEM analysis stabilizes after six subjects for this particular study.

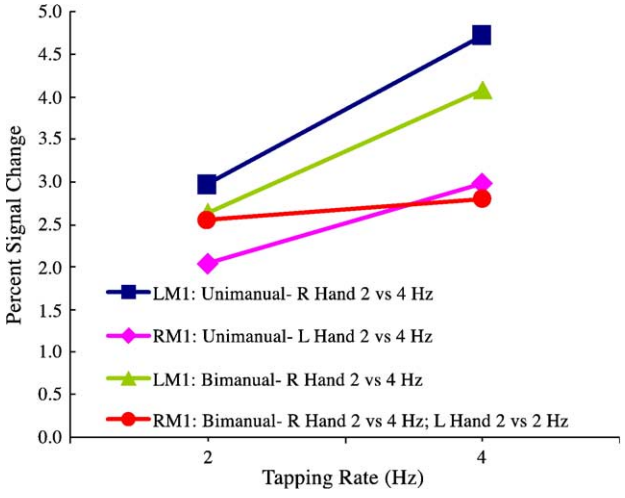

Fig. 6. Intersubject averaged MI activations vs. tapping rate. Blue line: The linear tendency of BOLD signal from LMI at unimanual task, according to movement rate. Purple line: The linear tendency of BOLD signal from RMI at unimanual task. Green line: The linear tendency of BOLD signal from LMI at bimanual task, which corresponded to right hand's movement between 2 and 4 Hz. Red line: The BOLD signal from RMI at bimanual task, which corresponded to left hand's consistent movement at 2 Hz, but shown respectively with right hand's switching between 2 and 4 Hz.

Discussion

In confirmatory studies (Büchel and Friston, 1997; Grafton et al., 1994; Maguire et al., 2001; McIntosh and Gonzalez-Lima, 1994), only a few selected models are usually examined in the structural equation estimations. Our exploratory approach, based on anatomic constraints, compares a large number of possible models and effectively avoids the possibility of missing the most appropriate model in the final result. The comparison between models themselves is a complicated procedure, and multiple statistical indices must be used (Hu and Bentler, 1999; MacCallum and Austin, 2000). Although different authors emphasize the importance of different indices, based on our observation, most of these indices yield very similar sorting orders among the models.

In this study, a validation of our exploratory approach was performed via a confirmatory analysis of resampled data. This analysis assessed the dependence on the number of subjects, given our experimental design, and the reproducibility of the ranking.

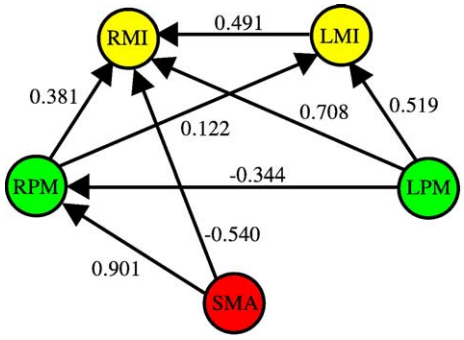

Fig. 7. The path map and weights for the best connectivity model in bimanual tasks.

Table 1
The path weight for each connectivity path in the final resulted bimanual model (Fig. 7)

Path	Path weight	Standardized path weight	Standard error	t value
LMI→RMI	0.147	0.491	0.018	8.260
RPM→RMI	0.368	0.381	0.059	6.288
LPM→RMI	0.822	0.708	0.146	5.623
SMA→RMI	−0.564	−0.540	0.138	4.092
RPM→LMI	0.392	0.122	0.285	1.374
LPM→LMI	2.014	0.519	0.344	5.862
LPM→RPM	−0.415	−0.344	0.231	1.801
SMA→RPM	0.978	0.901	0.208	4.713

Note. Standardized path weight: The path weights are standardized by the ratio of the standard deviations of the two connected variables, with the standard deviation of the causal variable constituting the denominator. This kind of standardized coefficient can express the relative response of the dependent variable for a standard deviation change in the explanatory variable.

Our results indicate that, with a large enough sample size, the selection of the best model is very stable (Table 3), demonstrating that the method is robust and we had a sufficient number of subjects for this study.

It is important to mention the issue of multiple comparisons in our method, which is a common pitfall in inference-based statistics. The issue is that we have a single data set to which we have applied more than 16,000 models. Based on chance alone, such a procedure is bound to produce significant models. Our approach is valid, then, only as an exploratory analysis. While our end result is a "best" model, this actually should be viewed as a hypothesis—generating result to be tested with new, independent data.

From the best-fitted model (Fig. 7), it can be seen that four paths are connected with right MI; one interpretation is that the left hand of these subjects is nondominant and requires more support from other motor related regions including right/left premotor areas and SMA. The interaction from left MI to right MI agrees well with the expected involvement of contralateral MI in bimanual coordination tasks. For example, Donchin et al. (1998) found unique cells in the monkey's primary motor cortex that were specifically activated with bimanual movements. Furthermore, the primary motor cortex has been observed to contain almost equal proportions of bimanually related neurons as the SMA (Donchin et al., 1998; Kazennikov et al., 1999; Kermadi et al., 1998). As in the GMP model, the dominant (right) hand may act as a "pace-maker" to drive the movement of the left hand, and this may be one cause of the temporal and spatial couplings. The finding here is also supported by previous studies of unimanual tasks, which revealed that the movement of the nondominant hand would also activate the dominant motor cortices, such as LMI (Kim et al., 1993).

Another important inference from our result is that the links between right PM and the two MIs play an important role in the temporal interference effect of bimanual coordination. The nature of interactions with bilateral MIs from the same PM area implies a source of disturbance in accuracy of bimanual performance, a notion that can be explained by the cross-talk model. If it is assumed that motor preparation in PM is a serial process, bimanual movements are prepared not simultaneously, but on a one-by-one basis. Some previous findings (Kurata, 1993; Sadato et al., 1997) suggest that the PMd may have a role in the integration of information, such as the sequence of finger movements, from other areas (e.g., SMA) to coordinate the left finger movements with that of its counterpart. According to the resultant best network map in the present study, the right premotor is perhaps the most likely candidate for the bottleneck of this serial preparation process in our task. The negative link from LPM to RPM can be interpreted by the conflicts of the motor preparations between the two PM areas, consistent with the intermanual cross-talk model. The result also agrees with the common presence of RPM in a number of functional imaging reports of bimanual motor coordination (De Weerd et al., 2003; Goerres et al., 1998; Immisch et al., 2001; Sadato et al., 1997).

The fact that SMA has functional paths pointing to RPM and RMI is perhaps related to its well-known role in motor planning, especially spatial planning. SMA is one of the structures revealed early on by imaging studies of bimanual tasks (Immisch et al., 2001; Jancke et al., 2000; Sadato et al., 1997; Stephan et al., 1999; Toyokura et al., 1999). The coupling between LMI and RMI has to be inhibited, probably resulting in the observed negative link from SMA to RMI. The link also agrees with the neuroanatomic findings that the PMd has dense cortico-cortical input from SMA (Koeneke et al., 2004; Kurata, 1991). Like most other reports, our present study does not distinguish between the right and left SMAs because they lie in close proximity and are not readily separable in fMRI. However, the asymmetry in the functional activation of the

Table 2
The overall fit indices for the best "probable" model (column A) and the best "improbable" model (column B) inferred by SEM

Model	A: Best "probable"	B: Best "improbable"
Goodness of fit index (GFI)	1.000	0.987
Adjusted goodness of fit index (AGFI)	0.9995	0.9243
Parsimony goodness of fit index (PGFI)	0.0667	0.165
χ^2/degree of freedom	0.00882	2.148
P value for χ^2	(0.925)	(0.143)
Root mean square error of approximation (RMSEA)	0.0	0.102
90% confidence interval for RMSEA	(0.0–0.08612)	(0.0–0.297)
P value for test of close fit (RMSEA < 0.05)	(0.935)	(0.197)
Largest standardized residual	0.0257	1.051
Normed fit index (NFI)	1.000	0.982
Parsimony normed fit index (PNFI)	0.100	0.327
Comparative fit index (CFI)	1.000	0.990

Table 3
The average Borda count from 1 to 6 subjects for reliability analysis of the best 5 models obtained in 7-subject data

Data size	Number of subsets	Model 1	Model 2	Model 3	Model 4	Model 5
1 subject	7	3.2857	2.2857	3.8571	3.4286	2.1429
2 subjects	21	3.4286	2.4286	3.0000	3.6667	2.4762
3 subjects	35	3.5724	2.5714	2.8857	3.6571	2.3143
4 subjects	35	3.9143	2.9143	2.9429	3.1714	2.0571
5 subjects	21	3.7143	2.7143	2.8095	3.5238	2.2381
6 subjects	7	4.7143	3.7143	3.2857	2.1429	1.1429

The highest-scoring model for each data size is highlighted.

left/right SMAs should be kept in mind and may be detectable in future fMRI studies with higher spatial resolution.

Of course, the bimanual motor activity also involves subcortical structures, particularly basal ganglia and cerebellum. In this study, we focused only on the cortical areas involved in the bimanual task to reduce the model complexity. Even though this model did not include all involved regions, as with any SEM study that examines effective connectivity, its results are still relevant because any covariance between cortical regions mediated by subcortical structures would be indirectly reflected in our cortical model. Furthermore, for demonstrating the utility of exploratory SEM, this cortical model is sufficient. Nonetheless, in interpreting our results, one should keep in mind the limitation of the ROIs.

Conclusion

Exploratory SEM analysis was applied to investigate the coupling mechanism between cortical motor areas in bimanual coordination. Given all probable models with connections between left/right MI, left/right PMdc (caudal dorsal premotor area), and SMA (supplementary motor area), the exploratory analysis was able to find a "best" model, which was confirmed to be reproducible across data subsets. The present study demonstrates the capability of SEM for exploring candidate models of effective connectivity related to a neuronal task to provide the best model for hypothesis testing of more extensive experimental data. The "best" model exhibits positive interactions from left MI to right MI, from left/right PMs to both MIs, and from SMA to right MI and right PM, and a negative link from left PM to right PM. This result is consistent with previous models of bimanual coordination.

Acknowledgments

This work was supported by the National Institutes of Health (Grants R01EB002009 and RO1EB000331), the Georgia Research Alliance, the Whitaker Foundation, and National Natural Science Foundation of China (Grant 39800049).

References

Baker, J.T., Donoghue, J.P., Sanes, J.N., 1999. Gaze direction modulates finger movement activation patterns in human cerebral cortex. J. Neurosci. 15, 10044–10052.

Büchel, C., Friston, K.J., 1997. Modulation of connectivity in visual pathways by attention: cortical interactions evaluated with structural equation modelling and fMRI. Cereb. Cortex 7, 768–778.

Byrne, B.M, 1994. Structural Equation Modeling and EQS and EQS Windows: Basic Concepts, Applications, and Programming. Sage Publications, Thousand Oaks, CA.

Cardoso de Oliveira, S., 2002. The neuronal basis of bimanual coordination: recent neuro-physiological evidence and functional models. Acta Psychol. 110, 139–159.

Chan, T., Chan, K., 1995. Effect of frequency ratio and environmental information on spatial coupling: a study of attention. Ecol. Psychol. 7 (2), 125–144.

Debaere, F., Wenderoth, N., Sunaert, S., Van Hecke, P., Swinnen, S.P., 2003. Internal vs. external generation of movements: differential neural pathways involved in bimanual coordination performed in the presence and absence of augmented visual feedback. NeuroImage 19, 764–776.

Debaere, F., Wenderoth, N., Sunaert, S., Van Hecke, P., Swinnen, S.P., 2004. Cerebellar and premotor function in bimanual coordination: parametric neural responses to spatiotemporal complexity and cycling frequency. NeuroImage 21, 1416–1427.

De Weerd, P., Reinke, K., Ryan, L., McIsaac, T., Perschler, P., Schnyer, D., Trouard, T., Gmitrof, A., 2003. Cortical mechanisms for acquisition and performance of bimanual motor sequences. NeuroImage 19, 1405–1416.

Donchin, O., Gribova, A., Steinberg, O., Bergman, H., Vaadia, E., 1998. Primary motor cortex in involved in bimanual coordination. Nature 395, 274–278.

Dum, R.P., Strick, P.L., 1991. The origin of corticospinal projections from the premotor areas in the frontal lobe. J. Neurosci. 11, 667–689.

Dym, C.L., Wood, W.H., Scott, M.J., 2002. Rank ordering engineering designs: pairwise comparison charts and borda counts. Res. Eng. Design 13, 236–242.

Franz, E.A., Zelaznik, H.N., McCabe, G., 1991. Spatial topological constraints in a bimanual task. Acta Psychol. 77, 137–151.

Gerbing, D., Anderson, J., 1993. Monte Carlo evaluations of goodness-of-fit indices. In: Bollen, K.A., Long, J.S. (Eds.), Testing Structural Equation Models. Sage Publications, Newbury Park, CA, pp. 40–65.

Grafton, S.T., Sutton, J., Couldwell, W., Lew, M., Waters, C., 1994. Network analysis of motor system connectivity in Parkinson's disease: modulation of thalamocortical interactions after pallidotomy. Hum. Brain Mapp. 2, 45–55.

Goerres, G.W., Samuel, M., Jenkins, I.H., Brooks, D.J., 1998. Cerebral control of unimanual and bimanual movements study: an H2(15)O PET. NeuroReport 9, 3631–3638.

Hu, L., Bentler, P.M., 1999. Cutoff criteria for fit indexes in covariance structure analysis: conventional criteria versus new alternatives. Struct. Equ. Modelling 6, 1–55.

Immisch, I., Waldvogel, D., VanGelderen, P., Hallett, M., 2001. The role of the medial wall and its anatomical variations for bimanual antiphase and in-phase movements. NeuroImage 14, 674–684.

Jancke, L., Peters, M., Himmelbach, M., Noesselt, T., Shah, J., Steinmetz, H., 2000. fMRI study of bimanual coordination. Neuropsychologia 38, 164–174.

Jirsa, V.K., Fuchs, A., Kelso, J.A.S., 1998. Connecting cortical and behavioral dynamics: bimanual coordination. Neural Comput. 10, 2019–2045.

Kazennikov, O., Hyland, B., Corboz, M., Babalian, A., Rouiller, E.M., Wiesendanger, M., 1999. Neural activity of supplementary and primary motor areas in monkeys and its relation to bimanual and unimanual movement sequences. Neuroscience 89, 661–674.

Kelso, J.A.S., Scholz, J.P., Schöner, G., 1988. Dynamics governs switching among patterns of coordination in biological movement. J. Exp. Psychol. Hum. Percept. Perform. 5, 229–238.

Kermadi, I., Liu, Y., Tempini, A., Calciati, E., Rouiller, E.M., 1998. Neuronal activity in the primate supplementary motor area and the primary motor cortex in relation to spatio-temporal bimanual coordination. Somatosens. Motor Res. 15, 287–308.

Kim, S.G., Ashe, J., Hendrich, K., Ellermann, J.M., Merkle, H., Ugurbil, K., Georgopoulos, A.P., 1993. Functional magnetic resonance imaging of motor cortex: hemispheric asymmetry and handedness. Science 261 (5121), 615–617.

Koeneke, S., Lutza, K., Wüstenberg, T., Jäncke, L., 2004. Bimanual versus unimanual coordination: what makes the difference? NeuroImage 22, 1336–1350.

Kurata, K., 1991. Corticocortical inputs to the dorsal and ventral aspects of the premotor cortex of macaque monkeys. Neurosci. Res. 12, 263–280.

Kurata, K., 1993. Premotor cortex of monkeys: set- and movement-related activity reflecting amplitude and direction of wrist movements. J. Neurophysiol. 69, 187–200.

MacCallum, R.C., Austin, J.T., 2000. Applications of structural equation modeling in psychological research. Annu. Rev. Psychol. 51, 201–226.

Maguire, E., Vargha-Khadem, F., Mishkin, M., 2001. The effects of

bilateral hippocampal damage on fMRI regional activations and interactions during memory retrieval. Brain 124 (6), 1156–1170.

Marteniuk, R.G., MacKenzie, C.L., 1980. Information processing in movement organization and execution. In: Nickerson, R. (Ed.), Attention and Performance VIII. Erlbaum, Hillsdale, pp. 29–57.

Mayville, J.M., Fuchs, A., Ding, M., Cheyne, D., Deecke, L., Kelso, J.A.S., 2001. Event-related changes in neuromagnetic activity associated with syncopation and synchronization timing tasks. Hum. Brain Mapp. 14, 65–80.

McIntosh, A.R., Gonzalez-Lima, F., 1994. Structural equation modeling and its application to network analysis in functional brain imaging. Hum. Brain Mapp. 2, 2–22.

Rao, S.M., Bandettini, P.A., Binder, J.R., Bobholz, J.A., Hammeke, T.A., Stein, E.A., Hyde, J.S., 1996. Relationship between finger movement rate and functional magnetic resonance signal change in human primary motor cortex. J. Cereb. Blood Flow Metab. 16, 1250–1254.

Roland, P.E., Zilles, K., 1996. Functions and structures of the motor cortices in humans. Curr. Opin. Neurobiol. 6, 773–781.

Sadato, N., Yonekura, Y., Waki, A., Yamada, H., Ishii, Y., 1997. Role of the supplementary motor area and the right premotor cortex in the coordination of bimanual finger movements. J. Neurosci. 17 (24), 9667–9674.

Schmidt, R.A., 1975. A schema theory of discrete motor skill learning. Psychol. Rev. 82, 225–260.

Stephan, K.M., Binkofski, F., Posse, S., Seitz, R.J., Freund, H.J., 1999. Cerebral midline structures in bimanual coordination. Exp. Brain Res. 128, 243–249.

Toyokura, M., Muro, I., Komiya, T., Obara, M., 1999. Relation of bimanual coordination to activation in the sensorimotor cortex and supplementary motor area: analysis using functional magnetic resonance imaging. Brain Res. Bull. 48, 211–217.

Tracy, J.I., Faro, S.S., Mohammed, F.B., Pinus, A.B., Madi, S.M., Laskas, J.W., 2001. Cerebellar mediation of the complexity of bimanual compared to unimanual movements. Neurology 57, 1862–1869.

Treffer, P.J., Turvey, M.T., 1993. Resonance constraints on rhythmic movement. J. Exp. Psychol. Hum. Percept. Perform. 6, 1221–1237.

Tuller, B., Kelso, J.A.S., 1989. Environmentally-specified patterns of movement coordination in normal and split-brain subjects. Exp. Brain Res. 75, 306–316.

Wright, S., 1920. The relative importance of heredity and environment in determining piebald pattern of guinea pigs. Proc. Natl. Acad. Sci. U. S. A. 6, 320–332.

Yamanishi, J., Kawato, M., Suzuki, R., 1980. Two coupled oscillators as a model for the coordinated finger tapping by both hands. Biol. Cybern. 37, 219–225.

Zwicker, W., 1991. The voters' paradox, spin, and the Borda count. Math. Soc. Sci. 22, 187–227.